

# Supplementary Figures

## Methylome-based cell-of-origin modeling (Methyl-COOM) identifies aberrant expression of immune regulatory molecules in CLL

Justyna A. Wierzbinska<sup>1,2,3</sup>, Reka Toth<sup>1</sup>, Naveed Ishaque<sup>3</sup>, Karsten Rippe<sup>3,4</sup>, Jan-Philipp Mallm<sup>3,4</sup>, Lara Klett<sup>3,4</sup>, Daniel Mertens<sup>3,5</sup>, Thorsten Zenz<sup>6</sup>, Thomas Hielscher<sup>7</sup>, Marc Seifert<sup>8</sup>, Ralf Küppers<sup>8</sup>, Yassen Assenov<sup>1</sup>, Pavlo Lutsik<sup>1</sup>, Stephan Stilgenbauer<sup>9</sup>, Philipp M. Roessner<sup>10</sup>, Martina Seiffert<sup>10</sup>, John Byrd<sup>11</sup>, Christopher C. Oakes<sup>11,12</sup>, Christoph Plass<sup>1,3,#,§</sup>, Daniel B. Lipka<sup>3,13,14,15,#,§</sup>

### Affiliations:

<sup>1</sup> Division of Cancer Epigenomics, German Cancer Research Center (DKFZ), Heidelberg, Germany

<sup>2</sup> Faculty of Biosciences, Heidelberg University, Heidelberg, Germany

<sup>3</sup> The German Cancer Consortium (DKTK)

<sup>4</sup> Division of Chromatin Networks, DKFZ, Heidelberg, Germany

<sup>5</sup> Mechanisms of Leukemogenesis, DKFZ, Heidelberg, Germany

<sup>6</sup> Experimental Hematology Lab, University Hospital Zurich, Switzerland

<sup>7</sup> Biostatistics, DKFZ, Heidelberg, Germany

<sup>8</sup> Group Molecular Genetics, Essen University Hospital, Essen, Germany

23 <sup>9</sup> Department of Internal Medicine, Ulm University, Ulm, Germany

24 <sup>10</sup> Division of Molecular Genetics, DKFZ, Heidelberg, Germany

25 <sup>11</sup> Department of Internal Medicine, Division of Hematology, The Ohio State University,  
26 Columbus, USA

27 <sup>12</sup> Department of Biomedical Informatics, The Ohio State University, Columbus, USA

28 <sup>13</sup> Translational Cancer Epigenomics, Division of Translational Medical Oncology, German  
29 Cancer Research Center (DKFZ), 69120 Heidelberg, Germany

30 <sup>14</sup> National Center for Tumor Diseases (NCT), 69120 Heidelberg, Germany

31 <sup>15</sup> Faculty of Medicine, Medical Center, Otto-von-Guericke-University, 39120 Magdeburg,  
32 Germany

33

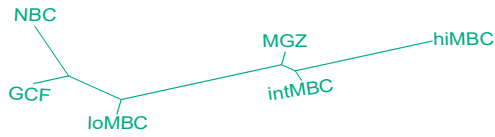
34 # Joint senior authors

35 § Corresponding authors

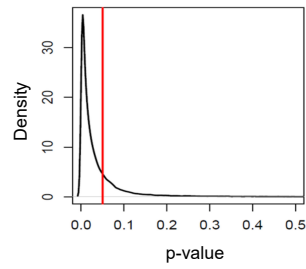
36

# Supplementary Figure 1

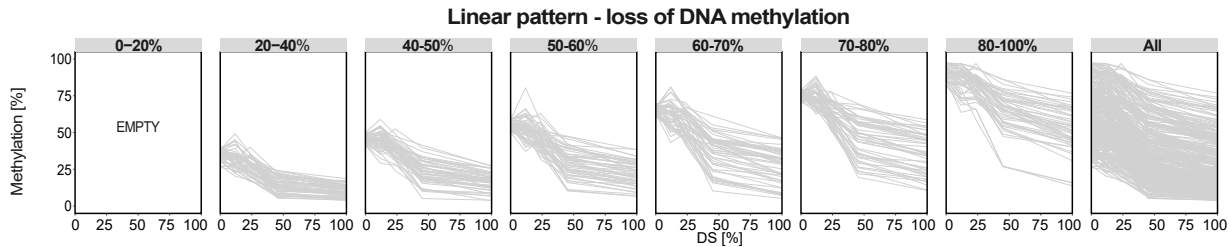
**a**



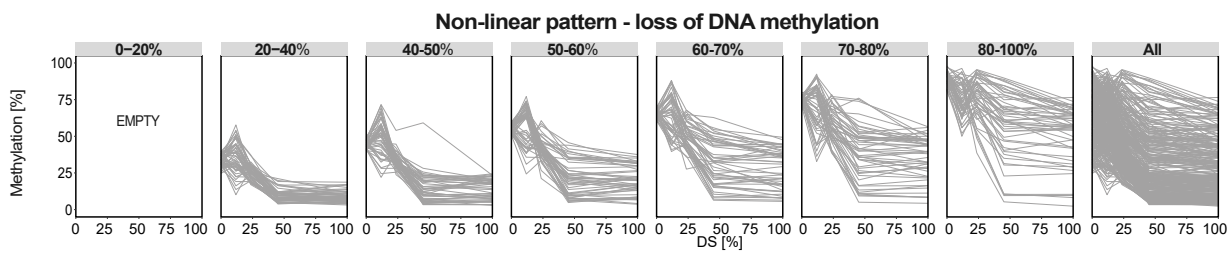
**b**



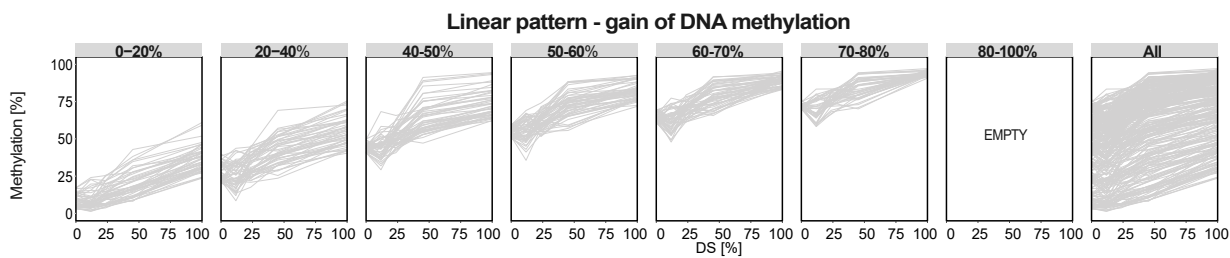
**c**



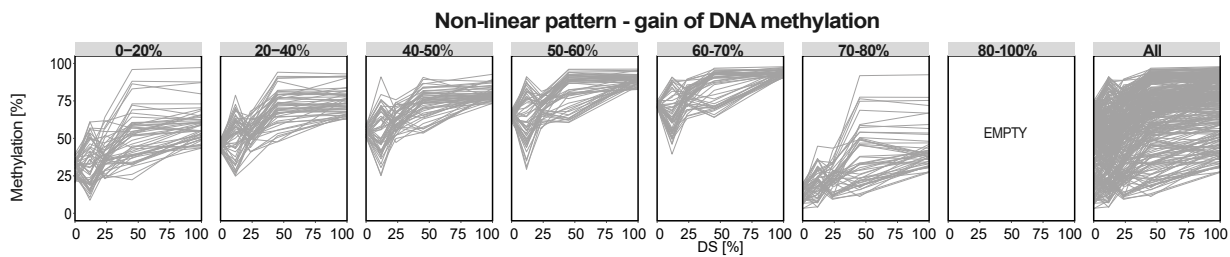
**d**



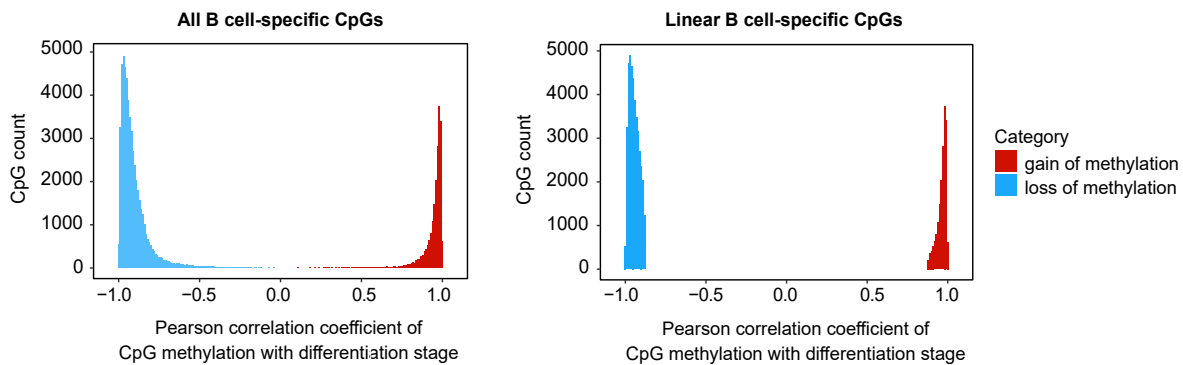
**e**



**f**



**g**



37 **Supplementary Figure 1. DNA methylation dynamics during normal B cell differentiation**  
38 **can be described by a linear model.**

39 **a) DNA methylation-based phylogenetic tree of normal B cell development.** The  
40 phylogenetic tree was generated using a set of CpG sites (total of 74,333CpGs, >20% DNA  
41 methylation change) that show dynamic DNA methylation changes during normal B cell  
42 differentiation (B cell-specific CpGs, minimum evolution method, R package ape). Manhattan  
43 pairwise distances between DNA methylation profiles of normal B cells at B cell-specific CpGs  
44 were used to determine the mode of methylation progression from naïve to memory B cell. Each  
45 branch represents a different B-cell subtype. NBC – naïve B cells; GCF –germinal center  
46 founder B cells; loMBC – early non-class switched memory B cells; intMBC – non class-  
47 switched memory B cells; sMGZ – splenic marginal zone B cells; hiMBC – class-switched  
48 memory B cells.

49 **b) Linear relationship between the differentiation stage of every B cell and the DNA**  
50 **methylation profiles at B cell-specific CpGs.** F-test statistics was used to test for linear  
51 relationship between the assigned differentiation stage for every B cell and the DNA methylation  
52 values at B cell-specific sites at a single CpG level. The vast majority of the B cell-specific CpGs  
53 (79.8%, 59,326 CpGs, p-value <0.05) showed linear DNA methylation dynamics across the six  
54 B cell differentiation stages. The y axis represents the density of B cell-specific CpG sites. The x  
55 axis represents p-values from F-test. The red line indicates p-value=0.05.

56 **c-f) Linearity of DNA methylation changes during normal B cell differentiation.** Absolute  
57 DNA methylation (Methylation [%]) was categorized into eight bins (0-20%; 20-40%, 40-50%;  
58 50-60%; 60-70%; 70-80%; 80-100%, all events) according to the DNA methylation status of  
59 naïve B cells. For each DNA methylation bin, 50 B cell-specific CpGs were randomly selected

60 from a total pool of 41,244 linear **(c)**, or 13,034 non-linear **(d)** B cell-specific CpGs that are  
61 losing methylation during B cell differentiation. For each DNA methylation bin with gain in  
62 methylation, 50 B-cell specific CpGs were randomly selected from a total pool of 18,102 linear  
63 **(e)**, or 1,973 non-linear **(f)** B cell specific CpGs. The y-axes represent absolute DNA methylation  
64 levels (%), while the x-axes depict the differentiation stage (DS) of normal B cells relative to  
65 hiMBCs.

66 **g) Histogram of Pearson correlation coefficients for DNA methylation status and**  
67 **differentiation stage of normal B cells.** Left panel: the histogram depicts the distribution of  
68 Pearson correlation coefficients for absolute DNA methylation levels with differentiation stage of  
69 all B cell-specific CpGs. Right panel: the histogram depicts the distribution of Pearson  
70 correlation coefficients for absolute DNA methylation levels with differentiation stage of linear B  
71 cell-specific CpG, only. Correlation is depicted depending on the direction of DNA methylation  
72 changes during B cell differentiation. DNA methylation loss (blue), DNA methylation gain (red).

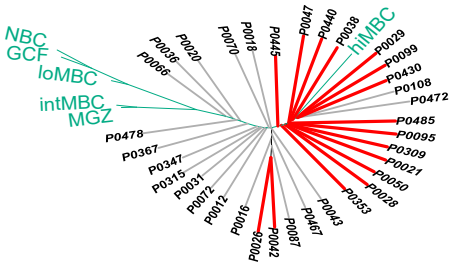
73

74

# Supplementary Figure 2

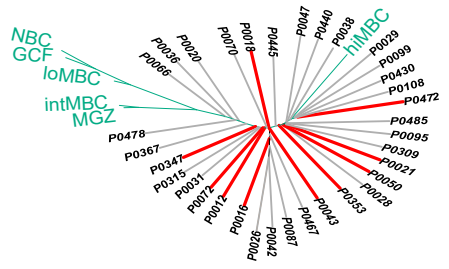
**a**

IGHV mut



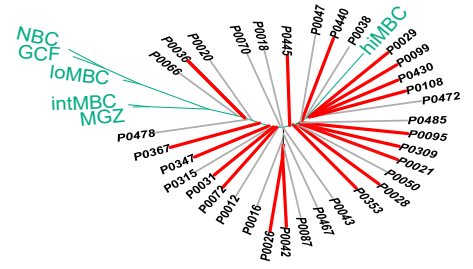
**b**

del17p



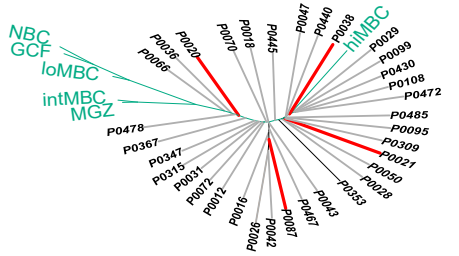
**c**

del13q14



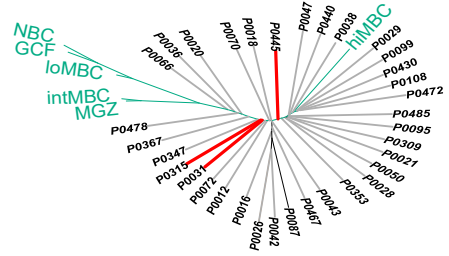
**d**

tri12



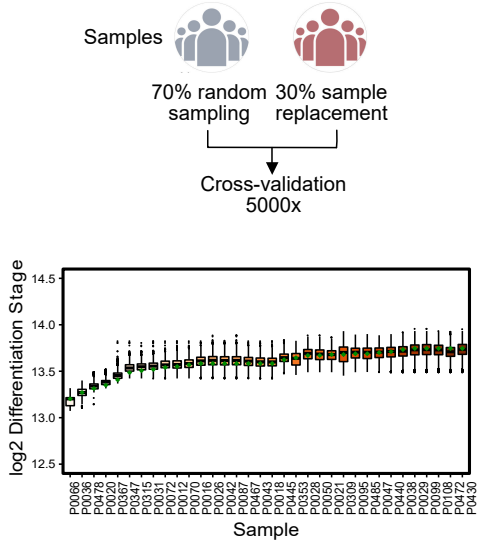
**e**

del11q

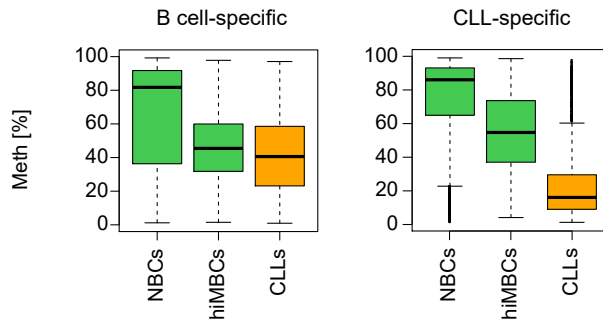


Mutation / Aberration  
■ yes ■ no

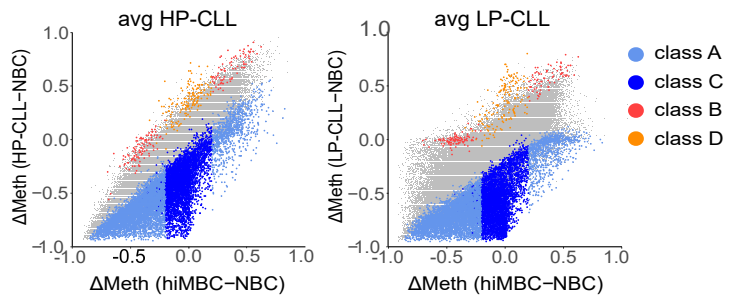
**f**



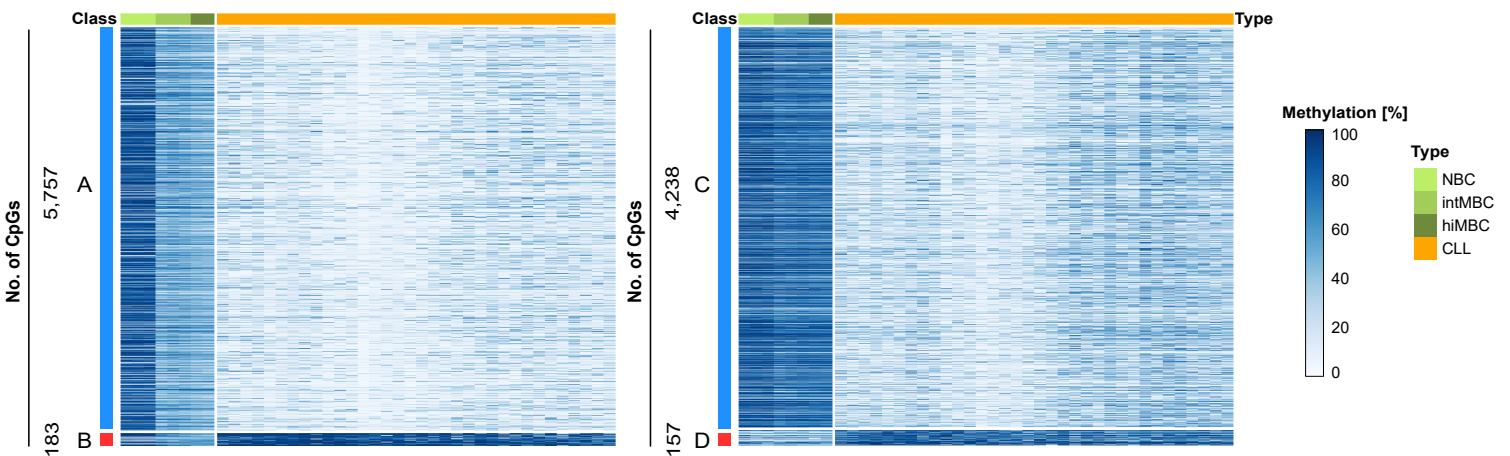
**g**



**h**



**i**



75 **Supplementary Figure 2. DNA methylation patterns of CLL in relation to normal B cell**  
76 **differentiation.**

77 **a-e) Identification of the cell-of-origin in CLL samples and their molecular/cytogenetic**

78 **status.** The presence of IGVH mutation (a), del17p (b), del13q14 (c), tri12 (d), del11q (e) are  
79 indicated in red, absence thereof in grey. Normal B cells are represented in green. NBCs - naïve  
80 B cells; GCFs – germinal center founder B cells; loMBCs – early non class-switched memory B  
81 cells; intMBCs – non class-switched memory B cells; sMGZs – splenic marginal zone B cells;  
82 hiMBCs – class-switched memory B cells (mature B cells).

83 **f) Robustness of the cell-of-origin assignment.** Bootstrapping (5000x) with a random sample

84 replacement was used to infer phylogenetic relationships and the closest normal B cell  
85 methylome (cell-of-origin) for every CLL sample. CLL patient cohort was repeatedly divided into  
86 two subgroups; 70% and 30% (5000 bootstraps). To minimize the likelihood of selection of the  
87 same sample multiple times, that would result in a bias towards few samples in the bootstrap  
88 analysis, a random sampling was allowed in the 70%-group, while sample replacement was  
89 restricted only to the 30%-group. The x axis represents CLL samples, the y axis denotes log<sub>2</sub>  
90 distances from the assigned cell-of-origin to NBCs (log<sub>2</sub> DS). Green points are representing the  
91 assign cell-of-origin using with the full CLL sample set (original assignment is represented in  
92 Supplementary Figure 1c).

93 **g) Net DNA methylation changes at B cell- and CLL-specific CpGs.** Left panel: net DNA

94 methylation change at B cell-specific CpGs for B cells (green) and CLL samples (orange). Right

95 panel: net DNA methylation change at CLL-specific CpGs for B cells (green) and CLL samples

96 (orange). The x-axes represent different cell types; NBCs – naïve B cells; hiMBCs - class-

97 switched memory B cells; CLL – chronic lymphocytic leukemia B cells. The y-axes denote  
98 absolute DNA methylation levels (%).

99 **h) CLL-specific DNA methylation events in the context of the classification by Oakes *et***

100 ***al.*** Differences in DNA methylation were represented from naive B cells to high-mature memory  
101 B cells (x-axis) and to CLLs (y-axis). Data for CpGs were averaged for each CLL subtype  
102 (average LP-CLL, average HP-CLL). CpGs were categorized as class A (light blue), class B  
103 (red), class C (dark blue), and class D (orange).

104 **i) Heatmap depicting absolute DNA methylation changes (Methylation, [%]) at CLL-**

105 **specific CpG sites.** Unsupervised hierarchical clustering of CLL-specific CpGs, class A and B  
106 sites (left), class C and D sites (right). The direction of DNA methylation change is indicated as  
107 blue and red bars for hypo- and hypermethylation, respectively. CLL samples are represented in  
108 orange. Normal B cells are represented in green (NBCs – naïve B cells; intMBC – non class-  
109 switched memory B cells, hiMBCs - class-switched memory B cells).

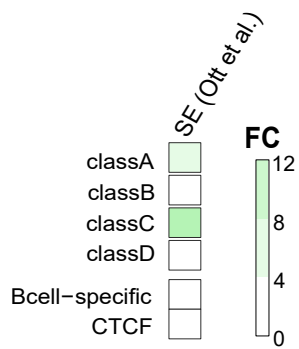
110

111

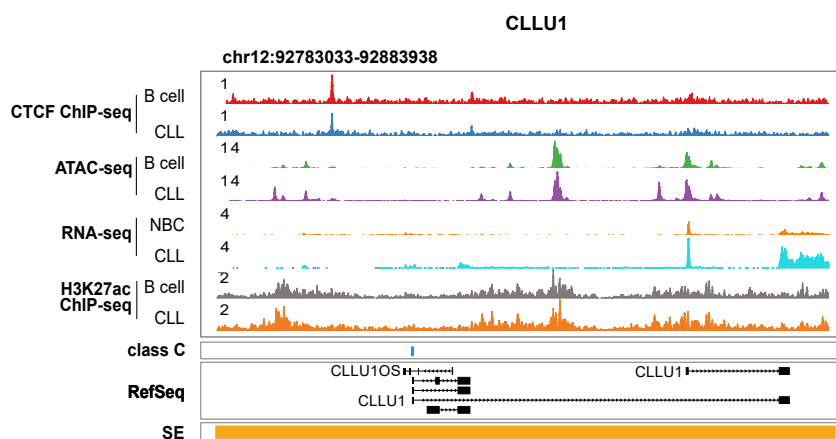
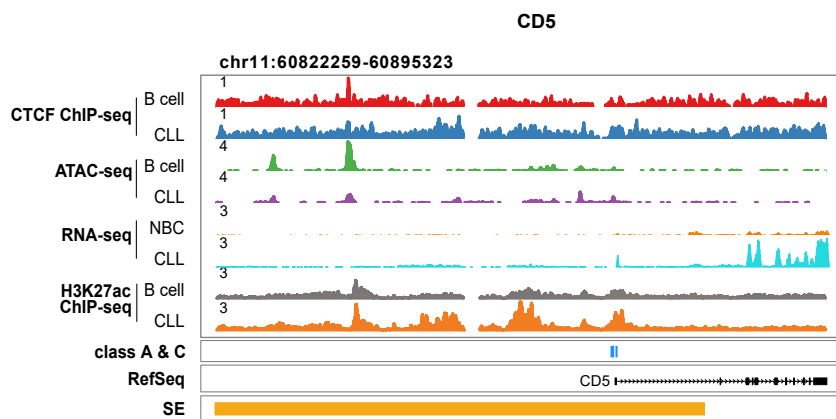


# Supplementary Figure 3

**a**



**b**



112 **Supplementary Figure 3. CLL-specific DNA methylation affects super-enhancers.**

113 **a) Enrichment of unified super-enhancer regions (SE) from Ott et al. in sequences**

114 **representing CLL-specific methylation** (PMID:30503705). Union of SEs was defined based  
115 on individual patient data in Ott et al. (n=18). Fold change (FC) was calculated using all 450k  
116 probes as a background. B-cell specific CpGs and CTCF motifs were used as controls.

117 **b) Locus plots of exemplary CLL-specific SE-associated genes.** CpG sites overlapping SEs

118 were associated with the closest gene and the correlation analysis between DNA methylation  
119 and gene expression was used to identify CLL-specific SE-associated genes. Locus plots  
120 include data from CTCF ChIP-seq on normal B cell (red) and CLL (blue); ATAC-seq on normal  
121 B cells (green) and CLL (purple); RNA-seq on normal B cells (orange) and CLL (cyan);  
122 H3K27ac on normal B cell (grey) and CLLs (orange). CLL-specific CpGs are annotated in blue.  
123 SE annotations are represented in orange.

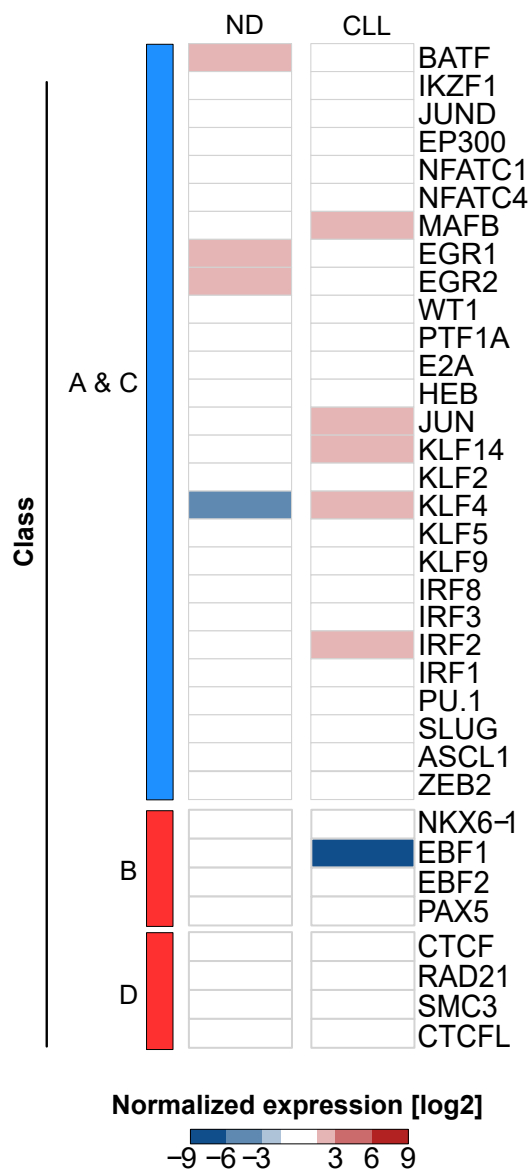
124

125

# Supplementary Figure 4

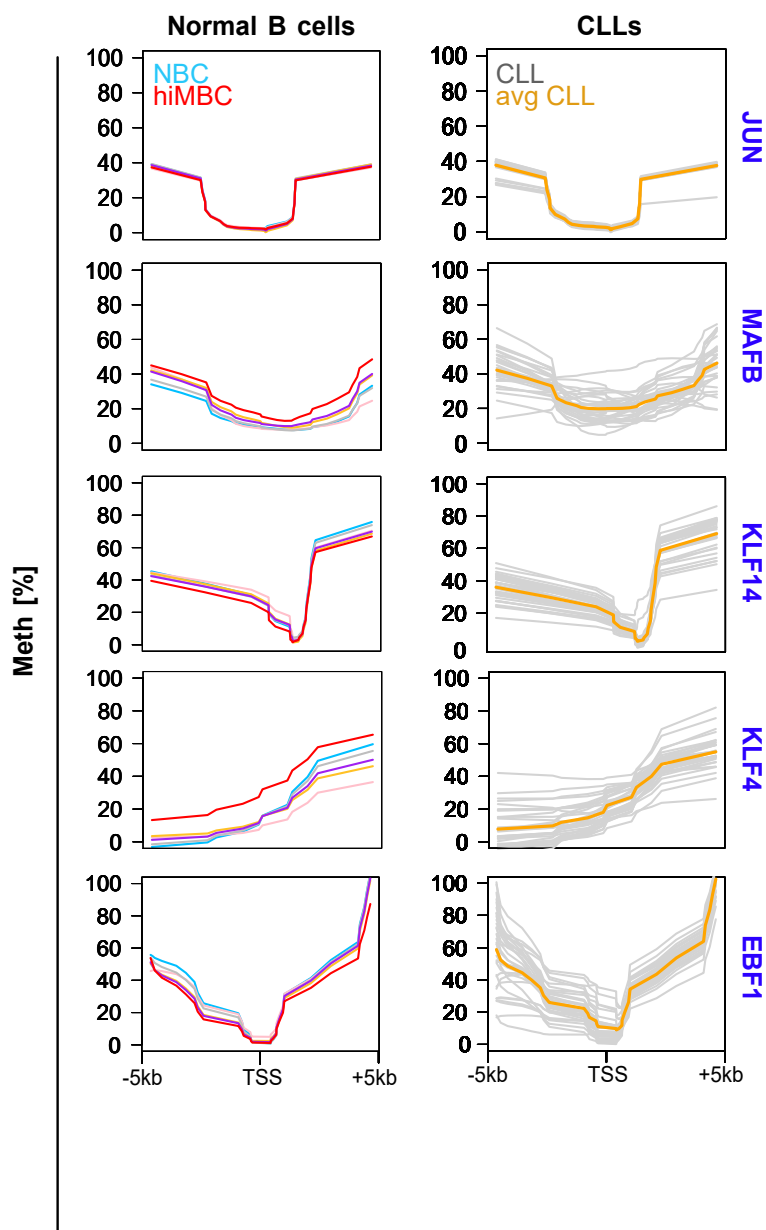
a

## TF expression levels



b

## Promoter DNA methylation



126 **Supplementary Figure 4. Aberrant TF programming in CLL.**

127 **a) Comparison of TF expression levels in CLL and in normal B cells.** TFs were selected  
128 based on the enrichment analysis presented in Figure 5d and 5e. Two different comparisons of  
129 expression patterns were represented, normal B cell differentiation-associated (ND,  $\Delta$ hiMBC-  
130 NBC), and CLL-associated (CLL;  $\Delta$ CLL-hiMBC). Normalized expression values were used (rlog  
131 normalization, log2). The direction of DNA methylation change observed at motif-associated  
132 CLL-specific CpG sites is indicated as blue and red bars for hypo- and hypermethylation,  
133 respectively.

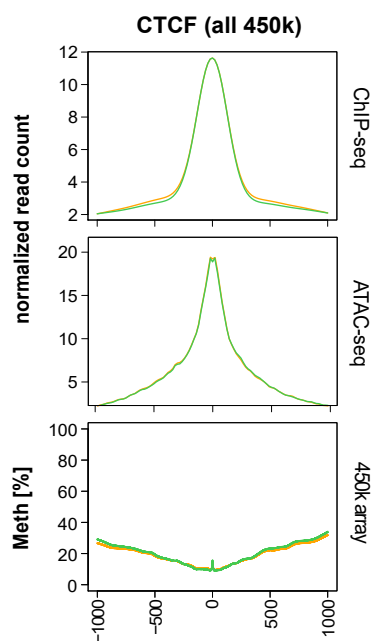
134 **b) DNA methylation profiles of promoters of differentially expressed TFs identified at**  
135 **CLL-specific CpG sites.** DNA methylation in the promoter regions is shown for six normal B  
136 cell subsets, representing different stages of B cell differentiation (left) and the CLL (right). NBC:  
137 naïve B cell; hiMBC – class-switched memory B cell; avg CLL – average DNA methylation  
138 change in CLL. The y-axis represents DNA methylation levels (%). The x-axis represents the  
139 transcription start site (TSS) +/-5kb.

140

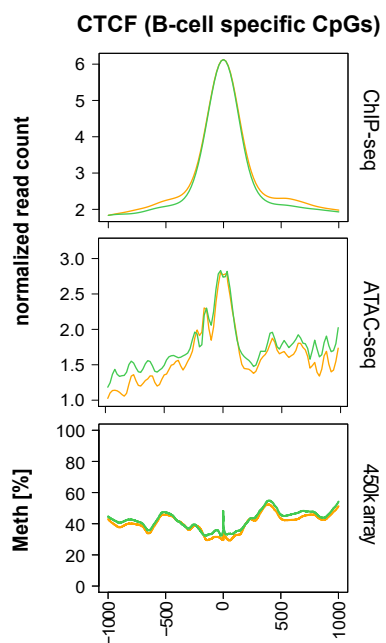
141

# Supplementary Figure 5

**a**



**b**



142 **Supplementary Figure 5. Aberrant CTCF programming in CLL.**

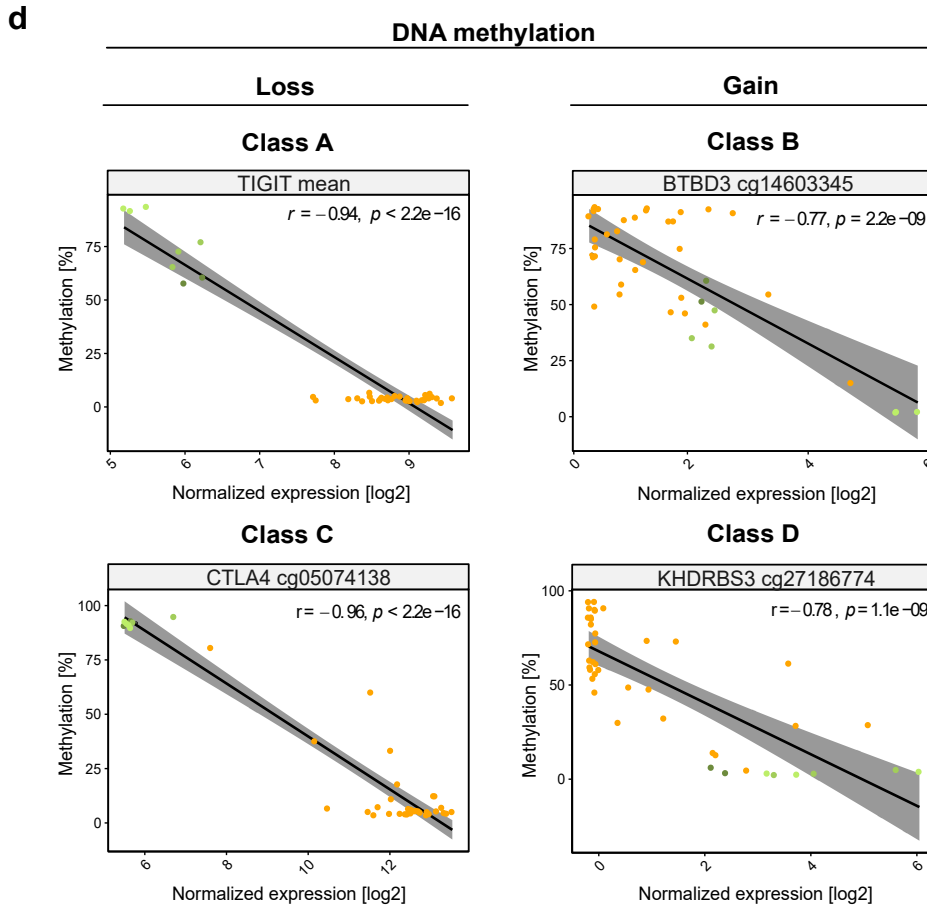
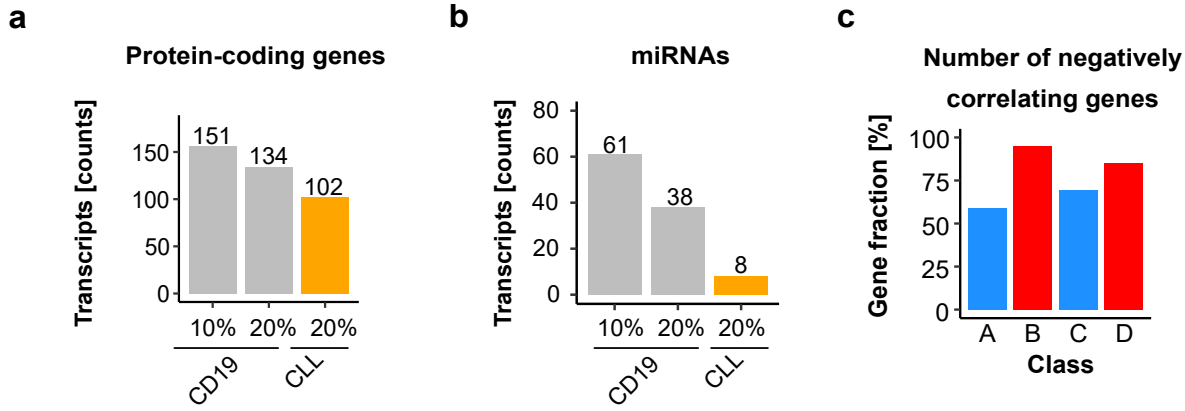
143 **a)** ATAC-seq and ChIP-seq read density and DNA methylation levels (%) at all 450k CpG  
144 probes co-locating with CTCF motifs (n=21,810 CpGs). Depicted are the genomic regions  
145 surrounding the CTCF motifs ( $\pm 400$ bp). CLL samples (n=7 CTCF ChIP-seq, n=18 ATAC-seq)  
146 are represented in orange, normal CD19<sup>+</sup> B cells (n=4 CTCF ChIP-seq, n=3 ATAC-seq) are  
147 depicted in green.

148 **b)** ATAC-seq and ChIP-seq read density and DNA methylation levels (%) at B cell-specific CpG  
149 sites co-locating with CTCF motifs (n=1,587 CpGs). Depicted are the genomic regions  
150 surrounding the CTCF motifs ( $\pm 400$ bp). CLLs (n=7 CTCF ChIP-seq, n=18 ATAC-seq) are  
151 represented in orange, normal CD19<sup>+</sup> B cells (n=4 CTCF ChIP-seq, n=3 ATAC-seq) are  
152 depicted in green.

153

154

# Supplementary Figure 6



155 **Supplementary Figure 6. Transcripts associated with CLL-specific aberrant DNA**  
156 **methylation.**

157 **a) Usage of CD19<sup>+</sup> B cells as a reference overestimates the number of CLL-specific**  
158 **protein-coding genes.** Differential DNA methylation between control B cells and CLL samples  
159 was calculated using different DNA methylation thresholds (10% or 20%). The bar plot  
160 illustrates the proportion of transcripts defined as CLL-specific using different control B cell  
161 sources (CD19<sup>+</sup> B cells are represented in grey, individual cell-of-origin is represented in  
162 orange). For CLL-specific protein coding genes, we used a correlation coefficient cutoff  $<-0.7$ .  
163 The numbers of uniquely identified CLL-specific genes are annotated on the top of the bars.

164 **b) Usage of CD19<sup>+</sup> B cells as a reference overestimates the number of CLL-specific**  
165 **microRNAs.** Differential DNA methylation between control B cells and CLL samples was  
166 calculated using different DNA methylation thresholds (10% or 20%). The bar plot illustrates the  
167 proportion of microRNAs defined as CLL-specific using different control B cell sources (CD19<sup>+</sup> B  
168 cells are represented in grey, individual cell-of-origin is represented in orange). For CLL-specific  
169 microRNAs we used an correlation coefficient cutoff  $\leq -0.35$ . The numbers of uniquely identified  
170 CLL-specific microRNAs are annotated on the top of the bars.

171 **c) Fraction of negatively correlating CLL-specific protein-coding genes.** DNA methylation  
172 at CLL-specific CpGs in the promoters of protein-coding genes was correlated with gene  
173 expression levels (Pearson correlation). Depicted is the percentage of negatively correlating  
174 genes (correlation coefficient  $r$ ,  $r < 0$ ).

175 **d) Exemplary correlation plots between CLL-specific DNA methylation and gene**  
176 **expression.** DNA methylation levels at promoter regions of protein-coding genes were  
177 correlated with the expression levels of associated genes. Examples for negative correlations

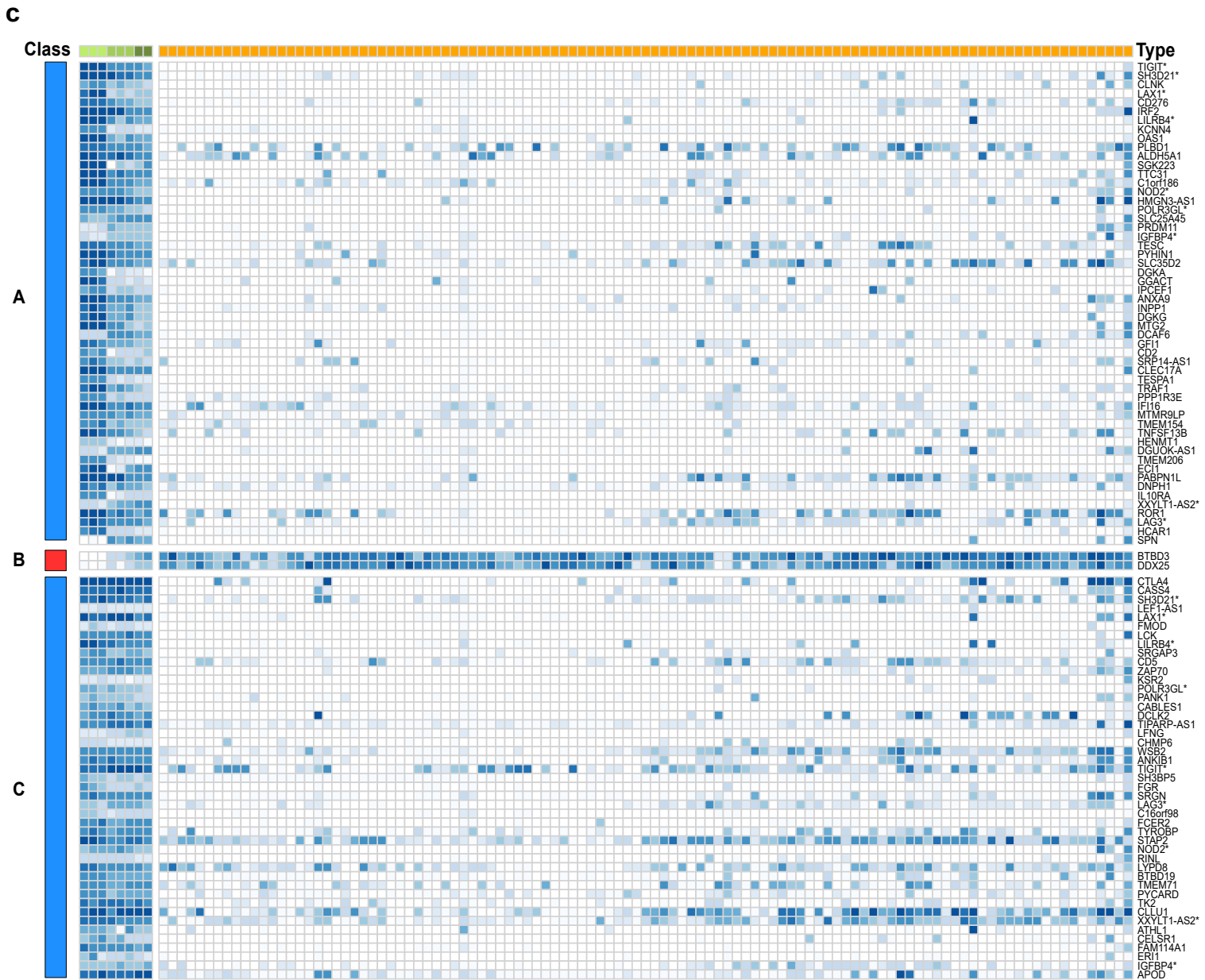
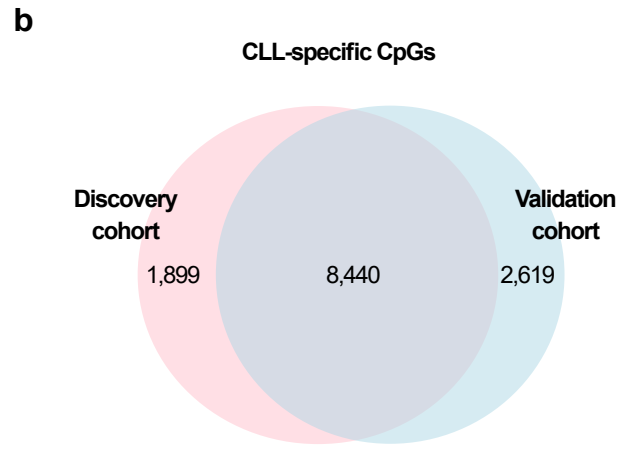
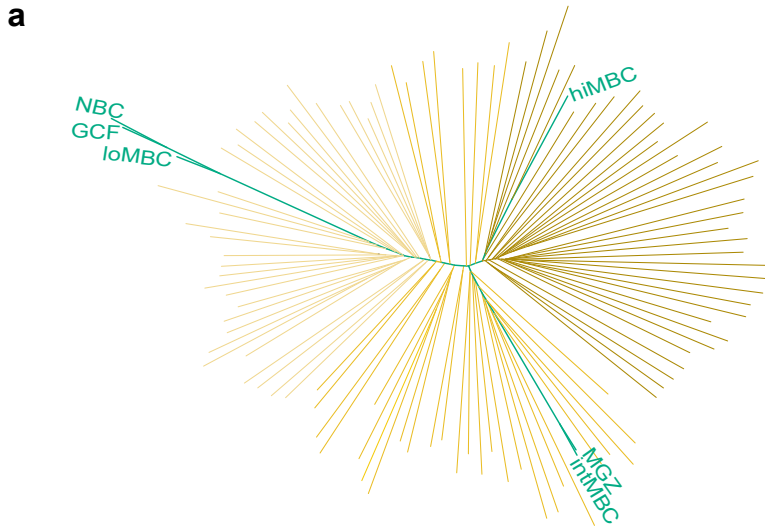


178 are represented for each class of CLL-specific CpGs. The x-axes depict gene expression levels  
179 (log<sub>2</sub> normalized counts) and the y-axes represent absolute DNA methylation [%]. Green:  
180 normal B cells. Orange: CLL samples.

181

182

# Supplementary Figure 7



183 **Supplementary Figure 7. Validation of CLL-specific DNA methylation events in an**  
184 **independent cohort of CLL patients.**

185 **a) Identification of the cell-of-origin in CLL samples using phylogenetic analysis.** The  
186 Methyl-COOM framework was applied to an independent cohort of CLL samples (Oakes et al.,  
187 Nat Genet 2016). Depicted is the phylogenetic tree that was generated using a set of linear CpG  
188 sites that show dynamic methylation changes during normal B cell differentiation as (linear B  
189 cell-specific CpGs, 59,326 CpGs). NBCs - naïve B cells; GCFs – germinal center founder B  
190 cells; loMBCs – early non class-switched memory B cells; intMBCs – non class-switched  
191 memory B cells; sMGZs – splenic marginal zone B cells; hiMBCs – class-switched memory B  
192 cells (mature B cells). The gradient color code of CLL samples corresponds to different levels of  
193 maturity reached by the cell-of-origin during the transformation event. CLL samples with a  
194 relatively immature cell-of-origin that are reprogrammed early during the differentiation process  
195 are represented in light orange color. CLLs with a cell-of-origin reprogrammed at a later stage of  
196 B cell differentiation are depicted in dark orange color. Normal B cells are represented in green.

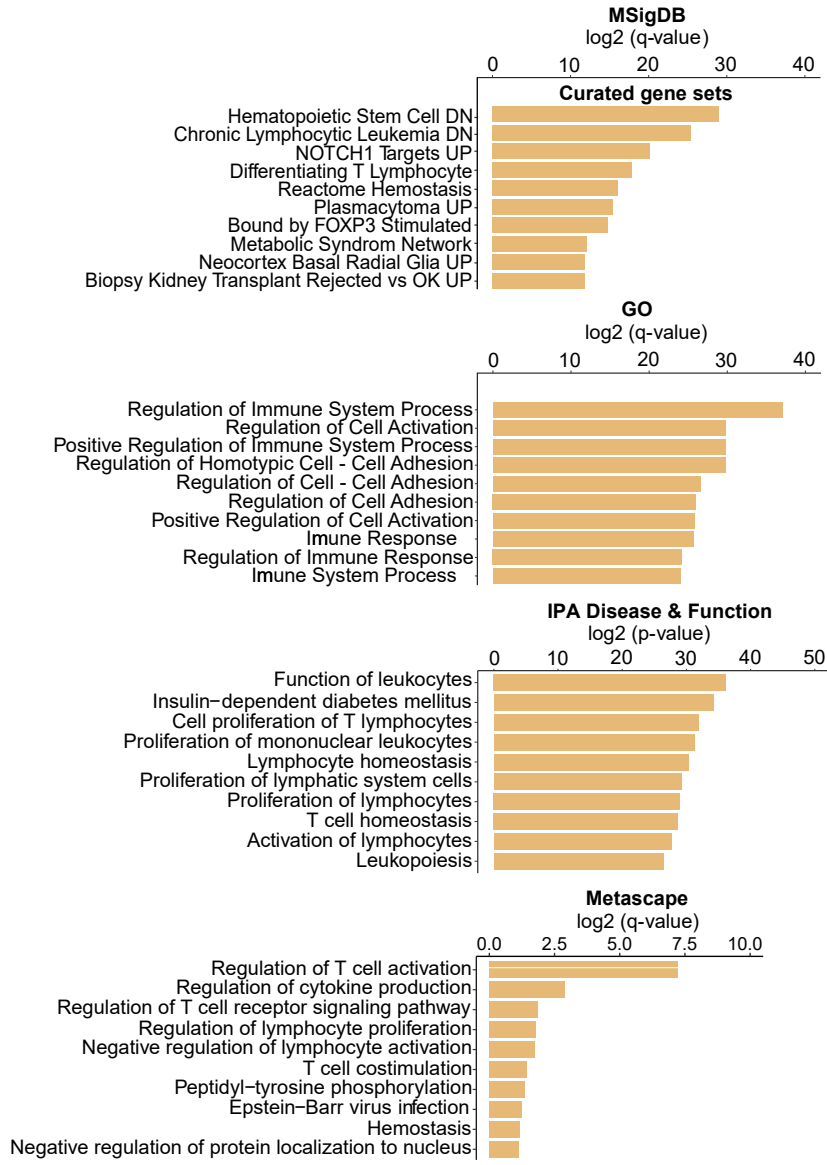
197 **b) High degree of concordance between CLL-specific CpGs identified in the discovery**  
198 **and validation cohorts.** The Venn diagram summarizes the overlap between the CLL-specific  
199 CpGs identified in the discovery (n=34 samples; 10,339 CpGs) and in the validation (n=107;  
200 11,029 CpGs) cohorts.

201 **c) Protein-coding genes associated with CLL-specific aberrant DNA methylation.**  
202 Heatmap depicting absolute DNA methylation levels [%] at CLL-specific CpG sites (classes A,  
203 B, C, and D) in the promoter regions of protein-coding genes. CLLs are represented in orange,  
204 normal B cells in green. Transcripts associated with more than one class of CLL-specific events  
205 in their promoter regions are marked with asterisks.

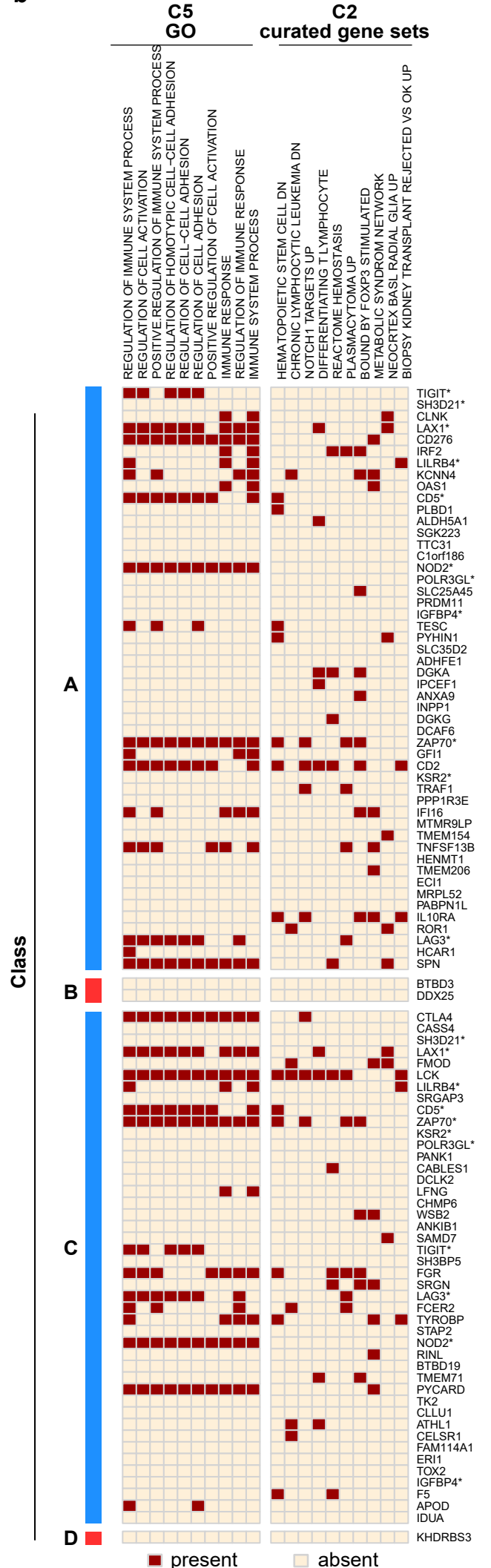
206

# Supplementary Figure 8

**a**



**b**



207 **Supplementary Figure 8. Transcripts associated with CLL-specific aberrant DNA**  
208 **methylation.**

209 **a) Functional enrichment analysis of CLL-specific protein-coding genes.** First panel:  
210 enrichment results from MSigDB 'Curated gene set'. Second panel: gene ontology (GO)  
211 enrichment analysis of CLL-specific epigenetically deregulated transcripts. Third panel:  
212 ingenuity (IPA) pathway disease & function enrichment. Fourth panel: metascape enrichment  
213 analysis of CLL-specific epigenetically deregulated transcripts

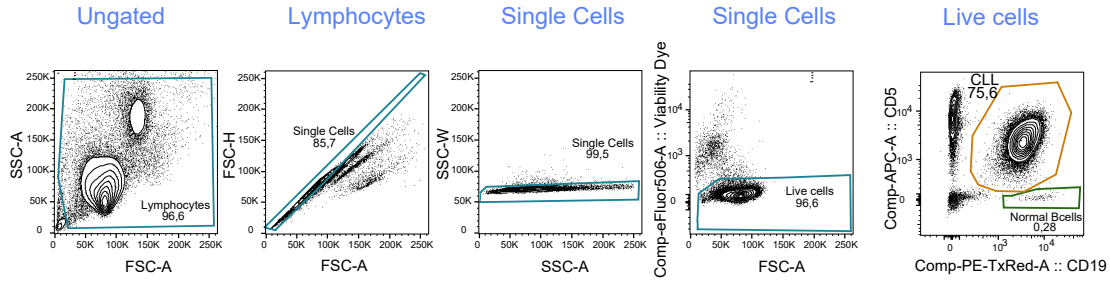
214 **b) Heatmap depicting results from MSigDB functional enrichment analysis of CLL-**  
215 **specific protein-coding genes.** MSigDB 'C2 Curated gene set' and MSigDB 'C5 GO analysis'.  
216 The direction of DNA methylation change is indicated on the left side of the heatmap in blue and  
217 red for hypo- and hypermethylation, respectively.

218

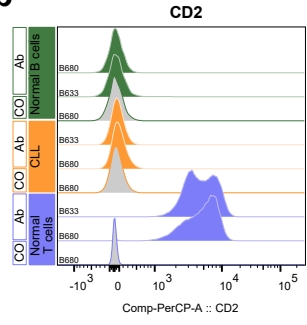
219

# Supplementary Figure 9

**a**



**b**



220 **Supplementary Figure 9. Flow cytometry analysis of B cells from CLL patients.**

221 **a) Gating strategy for the isolation of normal and malignant B cells from CLL patients.**

222 Normal B cells were identified by the sole expression of CD19<sup>+</sup>, while neoplastic B cells are  
223 positive for both CD19<sup>+</sup> and CD5<sup>+</sup>.

224 **b) Flow cytometry analysis of CD2.** Normal B cells ('Normal B cells'; CD19<sup>+</sup> B cells; green),  
225 CLL cells ('CLL', CD19<sup>+</sup> CD5<sup>+</sup> B cells; orange) and normal T cells ('Normal T cells', CD5<sup>+</sup> T cells,  
226 blue). 'Co', no antibody staining control; 'Ab', staining with an anti-CD2 antibody.